3 (forward primer 5′-CTTCCTGCCCTGTCCT-3′ and reverse primer 5′-CCCCATCCCATGCTATTCCAG-3′); and flanking the coding region of exon 4 except for the terminal three codons (forward primer 5′-GTTGCCAAACCGCCCTCTCCGT-3′ and reverse primer 5′-GCGGCCCTCAGGCCT-TGGTA-3′). The same PCR primers were used in the cycle-sequencing reaction with the fluorescence-based Applied Biosystems model 373A DNA-sequencing system.

14. Abbreviations for the amino acid residues are: A, Ala; C, Cys; D, Asp; E, Glu; F, Phe; G, Gly; H, His; I, Ile; K, Lys; L, Leu; M, Met; N, Asn; P, Pro; Q, Gln; R, Arg; S, Ser; T, Thr; V, Val; W, Trp; and Y, Tyr.
15. J. Reizer, A. Reizer, M. H. Saier, *Crit. Rev. Biochem. Mol. Biol.* **28**, 235 (1993).
16. DNA isolated from a phage containing the *aquaporin-2* cDNA (*9*) was digested with Eco RI and blunted with the Klenow fragment of DNA polymerase I [J. Sambrook, E. F. Fritsch, T. Maniatis, *Molecular Cloning: A Laboratory Manual* (Cold Spring Harbor Laboratory, Cold Spring Harbor, NY, 1989)]. The 860-bp insert was purified by gel electrophoresis and cloned into the Eco RV site between the 5′- and 3′-untranslated regions of the *Xenopus* β-globin gene in the expression vector T_7T_S (T_7T_SAQP-2), which is closely related to pSP64T [P. A. Krieg and D. A. Melton, *Nucleic Acids Res.* **12**, 7057 (1984)]. To introduce the R187C and the S216P mutations in our human *aquaporin-2* cDNA expression construct, we amplified genomic DNA of the patient with primers flanking exon 3 and exon 4 (*13*). A 65-bp Sau 3AI–Apo I fragment harboring the C to T transition at position 559 and a 174-bp Nar I–Kpn I fragment were isolated by gel electrophoresis and cloned between the Bam HI–Apo I sites and the Nar I–Kpn I sites, respectively, of pT_7T_SAQP-2. Clones pT_7T_SAQP-2RC and pT_7T_SAQP-2SP, which had nucleotide sequences identical to that of the wild-type *aquaporin-2* cDNA sequence (except for the transitions of C to T at position 559 and T to C at position 646), were selected by sequence analysis [M. Hattori and Y. Sakaki, *Anal. Biochem.* **162**, 232 (1986)]. In vitro transcription and capping were done with a linearized DNA template (1 μg) (Promega) according to the manufacturer's instructions, except that 1 mM final concentrations of nucleoside triphosphates and 7-methyl diguanosine triphosphate were used. Each cRNA was purified, dissolved in diethyl pyrocarbonate–treated H_2O, and its integrity determined by agarose gel electrophoresis. The RNA concentration was determined spectrophotometrically.
17. In vitro translation with wheat germ extracts was done as described [D. Scherly *et al.*, *EMBO J.* **8**, 4163 (1989)].
18. P. M. T. Deen *et al*, unpublished data.
19. R. Zhang and A. K. Verkman, *Am. J. Physiol.* **260**, C26 (1991).
20. We thank P. Krieg for the expression vector pT_7T_S. This study was supported by the Dutch Kidney Foundation (grants C91.1080, C92.1262, and C93.1299).

17 December 1993; accepted 25 January 1994

Stat3: A STAT Family Member Activated by Tyrosine Phosphorylation in Response to Epidermal Growth Factor and Interleukin-6

Zhong Zhong, Zilong Wen, James E. Darnell Jr.

The STAT family of proteins carries out a dual function: signal transduction and activation of transcription. A new family member, Stat3, becomes activated through phosphorylation on tyrosine as a DNA binding protein in response to epidermal growth factor (EGF) and interleukin-6 (IL-6) but not interferon γ (IFN-γ). It is likely that this phosphoprotein forms homodimers as well as heterodimers with the first described member of the STAT family, Stat91 (renamed Stat1α), which is activated by the IFNs and EGF. Differential activation of different STAT proteins in response to different ligands should help to explain specificity in nuclear signaling from the cell surface.

Interferon signaling to the cell nucleus operates through phosphorylation on tyrosine of proteins that we have termed STATs (for signal transducers and activators of transcription) (*1–5*). The first proteins in the family to be described were a 91-kD protein (an 84-kD form of this lacks 38 COOH-terminal amino acids) and a 113-kD protein (*1, 2*). With the discovery of the family members described here, we suggest that the proteins be named in order of their description. Thus, Stat1α and Stat1β are the 91-kD and 84-kD proteins and Stat2 is the 113-kD protein. After IFN-α treatment of cells, both Stat1 (α and β) and Stat2 become phosphorylated (*3*), whereas after IFN-γ treatment Stat1 (α and β) but not Stat2 is phosphorylated (*4*). Each ligand thus elicits a specific STAT response. Upon IFN-γ–induced activation, Stat1 (α or β) forms a homodimer that binds DNA. The dimer is formed by intermolecular interaction of Src homology 2 (SH2) regions with phosphotyrosine residues (*6*). It also seems likely that IFN-α promotes interactions of Stat1 with Stat2 through tyrosine phosphorylation (*3, 6*).

The discovery that other polypeptide ligands [including epidermal growth factor (EGF), platelet-derived growth factor (PDGF), colony-stimulating factor 1 (CSF-1), interleukin-10 (IL-10), ciliary neurotrophic factor (CNTF), and others] promote phosphorylation on tyrosine of Stat1 (*7–12*) raised the question of how transcriptional specificity might be maintained after cells encounter different ligands. Because the IFN-α and IFN-γ transcriptional response uses different STATs that share about 40% amino acid identity with each other (*2*), it seemed likely that additional family members might direct the formation of distinct DNA binding complexes in response to other signaling molecules. Indeed, CSF-1, IL-3, IL-4, IL-6, EGF, and CNTF all induce tyrosine phosphorylation of proteins or DNA binding activities that are distinct from the known Stat family members (*7–13*). Here, we describe a 92-kD mouse protein from the STAT family that is activated as a DNA binding protein by EGF and IL-6 but not by IFN-γ. We term this protein Stat3. A second family member, Stat4, has also been cloned by us and separately by others (*14, 15*).

We selected a 300-nucleotide probe (*16*) from the SH2 domain of the mouse Stat91 sequence by polymerase chain reaction and used this sequence to screen a mouse thymus complementary DNA (cDNA) library for clones representing possible family members. More than 10 such clones were partially sequenced, and all proved to be Stat1α or Stat1β. A number of placques that hybridized to the probe with less stringency were selected, subcloned, and sequenced (*14*). Of this group, about nine clones had identical sequences in the regions of overlap. This sequence was similar to but distinct from the Stat1 sequence. The longest clone contains both a stop codon and an ATG in a similar context compared to the translation start site of Stat1. With this ATG as a start codon, the new cDNA would encode a protein of 780 amino acids, similar in size to Stat1. The sequence of this cDNA, designated Stat3, had about 40 to 50% amino acid identity to Stat1 or Stat2, each of which is related to a similar degree (*2, 14*) (Fig. 1). In the same library screen, we also identified one other clone that is related but distinct from any of the above three genes and therefore named it Stat4. The complete sequences of Stat3, Stat4, and mouse Stat1 will appear elsewhere (*14, 17*).

Glutathione-S-transferase (GST) fusion products containing either 40 amino acids (amino acids 688 to 727) from the COOH-terminus or 158 amino acids (amino acids 2 to 159) from the NH_2-terminus of Stat3 were produced in bacteria, partially purified, and injected into rabbits to raise antisera (anti-Stat3c or anti-Stat3n, respectively) (*14*). From the A-431 or Hep-G2 cell extracts, the Stat3c antiserum precipitated predominantly a 92-kD protein and a less

Laboratory of Molecular Cell Biology, The Rockefeller University, New York, NY 10021, USA.

prominent band at 89 kD, both revealed by immunoblotting with the same antiserum (Fig. 2B). The same two bands were also detected in extracts of both murine and other human cell lines by immunoblotting with anti-Stat3c (*14*) and are likely to represent a major and a minor form of the Stat3 protein, but we cannot exclude at this point that the 89-kD protein is the protein product of a related gene. For clarity, we refer to the 92-kD protein as Stat3. Proteins were immunoprecipitated from extracts of cells treated with or without EGF, IL-6, and IFN-γ (*3*). After separation by electrophoresis, the proteins were blotted and tested for phosphotyrosine with a specific antibody. Both EGF and IL-6 led to tyrosine phosphorylation of a 92-kD protein that migrated in a manner identical to that of the precipitated Stat3 (Fig. 2A). The IFN-γ did not induce this phosphorylation (Fig. 2A) but did induce phosphorylation of Stat1 (Fig. 2C).

Both EGF and IFN-γ induce DNA binding by protein complexes that recognize the GAS (IFN-γ–activated site), for which the consensus sequence is TTNCNNNAA (*18*), or DNA elements that are similar to the consensus sequence of GAS. One such site is the hSIE, a mutant high-affinity version of the serum-inducible element (hSIE) from the c-*fos* promoter. This ~20-nucleotide element has an A substituted for a C in one position, making it conform closely to the GAS consensus and to bind more tightly to serum-induced factors (SIFs) (*7*, *19*). EGF treatment of A-431 cells activated proteins that formed three complexes with the hSIE, labeled SIF-A, SIF-B, and SIF-C (Fig. 3A). In contrast, IFN-γ induced only SIF-C (*7*). Treatment of Hep-G2 cells with IL-6 (30 ng/ml) induced an activity that formed one major complex with the same oligonucleotide that migrated indistinguishably from SIF-A (*7*) (Fig. 3A). These extracts were also tested for their ability to react with the native human SIE site, which is conserved in rodents and humans, and were compared directly to the synthetic hSIE element. After EGF treatment, weaker complexes with migration rates like those of SIF-A and SIF-B were observed with the native SIE sequence, but very little if any SIF-C was observed (Fig. 3A). SIF-A was also formed by the binding of proteins from nuclear extracts of the Hep-G2 cells treated with IL-6 to the native SIE site. All these DNA-protein interactions were sequence-specific, as the shifted bands disappeared when excess unlabeled oligonucleotide of the same sequence was included in the binding reactions. The induction of these DNA binding complexes apparently depended on tyrosine phosphorylation because genistein, a kinase inhibitor that blocks tyrosine phosphorylation (*20*), reduced the formation of the three complexes.

We also tested the EGF-induced complexes for reactivity with anti-Stat3 (Fig. 3B). Both SIF-B and SIF-A were specifically abolished by addition of anti-Stat3c. Two new bands, which were not present in the binding reactions with preimmune serum, appeared in the upper part of the gel when anti-Stat3c was added, which suggests that two supershifted species formed. Anti-Stat3n also blocked the formation of SIF-A and reduced the formation of SIF-B. SIF-C was unaffected by both antisera. The same result was obtained when formation of SIF-A was induced by EGF or by IL-6 (Fig. 3B). These data suggest that SIF-A and SIF-B both contain Stat3. Both SIF-B and SIF-C reacted with anti-Stat1α (*7*). Because SIF-B reacted with antibodies to Stat3 and to Stat1α and because SIF-C is known to be a Stat1α dimer (*6*), it appears that SIF-B could be a heterodimeric complex between Stat1α and Stat3. Likewise, SIF-A is likely to contain a homodimer of Stat3.

To confirm that the gel-shift pattern could be attributed to the Stat3 protein and

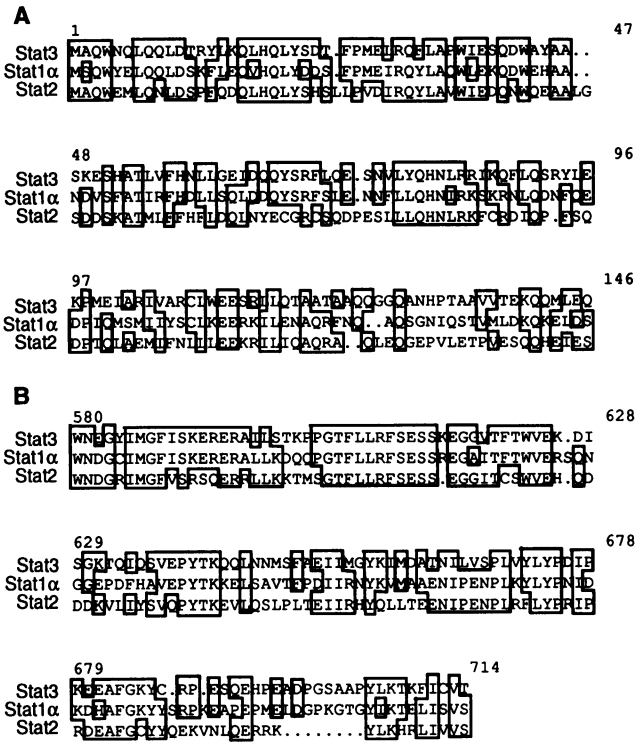

Fig. 1. Amino acid sequences for mouse Stat3 and two human members of the Stat gene family. (**A**) Alignment of the amino acid sequences of the NH_2-terminus of the Stat proteins. (**B**) Alignment of the amino acid sequences of the putative SH2 domain of the Stat proteins. Amino acids that are conserved between members of the Stat gene family are boxed. Abbreviations for the amino acid residues are: A, Ala; C, Cys; D, Asp; E, Glu; F, Phe; G, Gly; H, His; I, Ile; K, Lys; L, Leu; M, Met; N, Asn; P, Pro; Q, Gln; R, Arg; S, Ser; T, Thr; V, Val; W, Trp; and Y, Tyr.

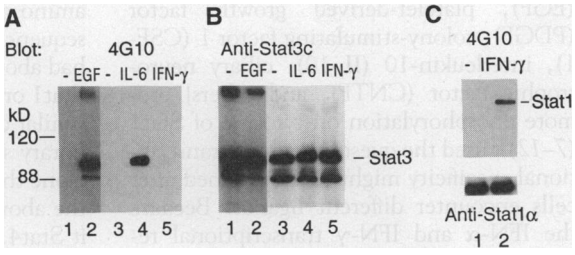

Fig. 2. Tyrosine phosphorylation of Stat3 in response to EGF and IL-6. (**A**) Protein immunoblot of anti-Stat3c precipitated with antibody to phosphotyrosine. Cell lysates were prepared from A-431 cells that were untreated (lane 1) or treated with EGF (Upstate Biotechnology; 100 ng/ml for 15 min) (lane 2) or from Hep-G2 cells that were untreated (lane 3), treated with IL-6 (Gibco-BRL; 30 ng/ml for 15 min) (lane 4), or treated with IFN-γ (*3*) (lane 5). Proteins in the lysates were immunoprecipitated with anti-Stat3c and separated by SDS–polyacrylamide gel electrophoresis (7% gel). The blot was then probed with an antibody specific to phosphotyrosine, 4G10 (1:1000; Upstate Biotechnology) (*5*). Prestained molecular size markers (Sigma) are indicated on the left. (**B**) Protein immunoblot with anti-Stat3c. The blot was stripped of the 4G10 antibody and probed with anti-Stat3c (1:1000). (**C**) As a control, extracts of Hep-G2 cells treated with IFN-γ were precipitated with anti-Stat1, subjected to electrophoresis, and stained with phosphotyrosine antibody to show phosphorylation of Stat1. The position where 92-kD Stat3 migrated is indicated on the right of (A) and (B). A-431 cells were grown in Dulbecco's modified Eagle's medium (DMEM) supplemented with 10% bovine calf serum. The cells were transferred to serum-free medium 24 hours before treatment with EGF. Hep-G2 cells were grown in 1:1 DMEM: Ham's F12 medium with 10% fetal calf serum. They were also serum-starved overnight before being treated with IL-6. Treatment with IFN-γ was as described (*3*).

not to a cross-reacting protein, we transfected COS-1 cells with an expression vector (Rc/CMV; Invitrogen) encoding either Stat3 or Stat4, expression of which was driven by a cytomegalovirus (CMV) promoter. As judged by protein immunoblotting with anti-Stat3c (*14*), lysates from cells transiently transfected with Rc/CMV-Stat3 contained at least 10 times more Stat3 than nontransfected COS-1 cells or COS-1 cells transfected with Rc/CMV-Stat4. Assuming at most a 10% transfection efficiency, this suggests an increase of Stat3 of at least a 100-fold in successfully transfected cells. Nuclear extracts from untransfected cells or cells transfected with Stat4 did not produce detectable SIF-A complexes in a gel mobility-shift analysis after EGF treatment. Weak activation of SIF-B and SIF-C complexes was observed (Fig. 4). Cells transfected with Rc/CMV-Stat3 and then treated with EGF, however, contained very large amounts of SIF-A, at least 100 times the amount in control nuclear extracts. The abundance of SIF-B was also increased in cells transfected with Stat3 relative to that in cells that were not transfected or that were transfected with Stat4 (Fig. 4). The SIF-A and SIF-B complexes from the Stat3-transfected COS cells migrated indistinguishably from the endogenous DNA binding protein activated in A-431 cells, and both complexes were supershifted by anti-Stat3c (Fig. 4, lane 8). The phosphorylated Stat3 induced by EGF in the transfected COS-1 cells also formed two distinctive DNA binding complexes that recognized the natural serum response element in the c-*fos* promoter (Fig. 4).

Our results indicate that the STAT family of proteins includes a number of different members through which growth factors can differentially modulate gene transcription. Stat3 is activated by both EGF and IL-6 but not by IFN-γ and can bind DNA in the absence of Stat1α or Stat2. The DNA binding SIF-B apparently contains both Stat1 and Stat3, possibly as heterodimers. The transcriptional activation potential of the different complexes remains to be determined. The α_2 macroglobulin gene is transcriptionally activated by IL-6, and the most important DNA binding element [TT(C/A)CNG(G/T)AA] resembles the TTNCNNNAAA consensus sequence found in all the IFN-γ–inducible genes (*18, 21*). An 89-kD DNA binding protein recognizes the α_2 macroglobulin element and is phosphorylated on tyrosine but does not precipitate with anti-Stat1 (*22*). The IL-6–induced phosphoprotein observed here is likely Stat3.

From our results, it appears that a series of sequences similar to the GAS sequence may bind a group of closely related STAT proteins. Specificity in response is probably not absolute but may depend on the relative concentrations of Stat1 and Stat3 and the affinity of homo- and heterodimers of these proteins for sites in the EGF-, IL-6– and IFN-γ–dependent genes. An important unsolved question for the moment is how many distinct ligand-dependent response

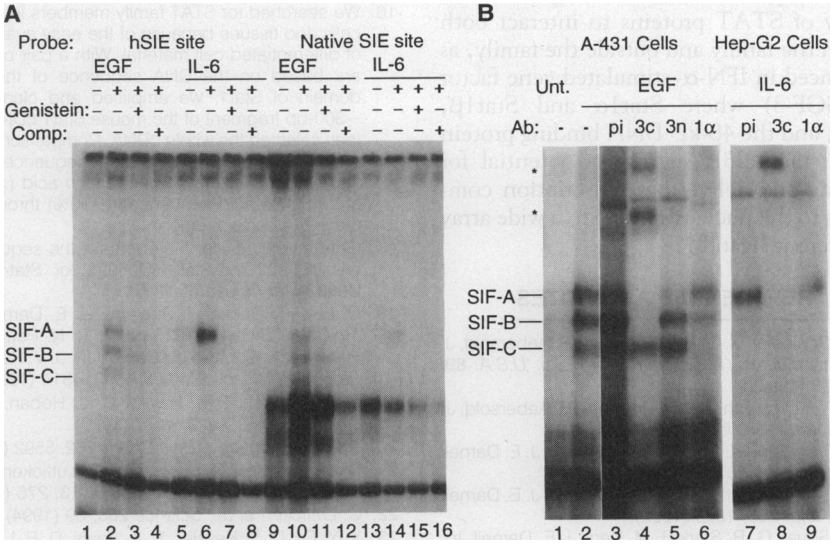

Fig. 3. The presence of Stat3 in SIF DNA binding complexes. (**A**) Activation of sequence-specific DNA binding proteins (*7*) through tyrosine phosphorylation induced by EGF and IL-6. Gel mobility-shift analysis of nuclear extracts was done with labeled oligonucleotide probes with either a high-affinity SIE sequence (hSIE; double-stranded GTCGACATTTCCCGTAAATCGTCGA) (*7, 19*) (lanes 1 to 8) or a native c-*fos* SIE sequence (double-stranded GTCGACAGTTCCCGTCAATCGTCGA) (*19*) (lanes 9 to 16). Nuclear extracts were prepared from serum-starved A-431 cells that were untreated (lanes 1 and 9), treated with EGF (100 ng/ml) for 15 min (lanes 2, 4, 10, and 12), or treated with genistein (100 μg/ml) (Gibco-BRL) for 2 hours before EGF treatment (lanes 3 and 11). Nuclear extracts were also prepared from Hep-G2 cells growing in serum-free medium that were untreated (lanes 5 and 13), treated with IL-6 (30 ng/ml) for 15 min (lanes 6, 8, 14, and 16), or treated with genistein for 2 hours before IL-6 treatment (lanes 7 and 15). An excess (100 times the amount of labeled oligonucleotide) of unlabeled hSIE (lanes 4 and 8) or of native c-*fos* SIE (lanes 12 and 16) oligonucleotide was added in the indicated binding reactions (Comp). The migration of SIF-A, SIF-B, and SIF-C is indicated on the left. (**B**) Detection of Stat3 in SIF-A and SIF-B. A-431 cells were untreated (Unt.) (lane 1) or treated with EGF as above (lanes 2 through 6). Hep-G2 cells were treated with IL-6 as above (lanes 7 through 9). Gel mobility-shift assays were done with nuclear extracts that had been reacted with 0.5 μl of preimmune (pi) serum (lanes 3 and 7), anti-Stat3c (lanes 4 and 8), anti-Stat3n (lane 5), or anti-Stat1α (lanes 6 and 9). Ab, antibody. The migration of SIF-A, SIF-B, and SIF-C is indicated at the left. Asterisks denote the positions of the supershifted species.

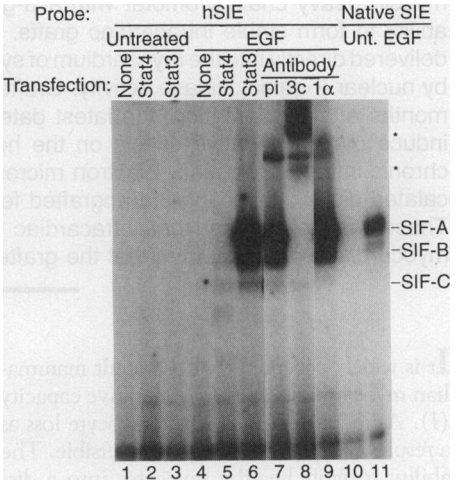

Fig. 4. Enhanced response to EGF in cells that overexpress Stat3. Gel mobility-shift analyses were done (Fig. 3) with nuclear extracts prepared from COS-1 cells that were untransfected (lanes 1 and 4) or transfected with Rc/CMV-Stat4 (lanes 2 and 5) or with Rc/CMV-Stat3 (lanes 3 and 6 through 11). COS cells were untreated (lanes 1 through 3 and 10) or treated with EGF (100 ng/ml for 15 min; lanes 4 through 9 and 11). Preimmune serum (0.5 μl) (lane 7), anti-Stat3c (lane 8), or anti-Stat1α (lane 9) was included in the indicated binding reactions. Either hSIE (lanes 1 through 9) or native SIE (lanes 10 and 11) oligonucleotide probes were used in the gel mobility-shift assays. The positions where SIF-A, SIF-B, and SIF-C migrated are indicated on the right of the gel. Asterisks at the right denote the positions of the supershifted species. We made plasmids Rc/CMV-Stat3 and Rc/CMV-Stat4 by inserting the complete coding sequences of Stat3 and Stat4, respectively, into the Not I and Apa I sites of the expression vector Rc/CMV (Invitrogen, San Diego, California). COS-1 cells were grown as a monolayer in DMEM supplemented with 10% bovine calf serum and transfected by the calcium phosphate method (*24*). The cells were transferred to DMEM without serum 48 hours after transfection. Cells were treated with EGF (Fig. 2) 60 hours after transfection, and nuclear extracts were prepared (Fig. 3).

elements exist. The discovery of new members of the STAT family, coupled with potential heterodimer formation, considerably broadens the possible range of specific STAT responses to different ligands. This ability of STAT proteins to interact both within the family and outside the family, as evidenced in IFN-α–stimulated gene factor 3 (ISGF-3) where Stat1α and Stat1β, Stat2, and the 48-kD DNA binding protein all interact (*23*), suggests a potential for forming and delivering transcription complexes to the nucleus specific to a wide array of different ligands.

REFERENCES AND NOTES

1. C. Schindler, X.-Y. Fu, T. Improta, R. Aebersold, J. E. Darnell Jr., *Proc. Natl. Acad. Sci. U.S.A.* **89**, 7836 (1992).
2. X.-Y. Fu, C. Schindler, T. Improta, R. Aebersold, J. E. Darnell Jr., *ibid.*, p. 7840.
3. C. Schindler, K. Shuai, V. R. Prezioso, J. E. Darnell Jr., *Science* **257**, 809 (1992).
4. K. Shuai, C. Schindler, V. R. Prezioso, J. E. Darnell Jr., *ibid.* **258**, 1808 (1992).
5. K. Shuai, G. R. Stark, I. M. Kerr, J. E. Darnell Jr., *ibid.* **261**, 1744 (1993).
6. K. Shuai *et al.*, *Cell*, in press.
7. H. B. Sadowski, K. Shuai, J. E. Darnell Jr., M. Z. Gilman, *Science* **261**, 1739 (1993).
8. A. C. Larner *et al.*, *ibid.*, p. 1730.
9. O. Silvennoinen, C. Schindler, J. Schlessinger, D. E. Levy, *ibid.*, p. 1736.
10. S. Ruff-Jamison, K. Chen, S. Cohen, *ibid.*, p. 1733.
11. X.-Y. Fu and J.-J. Zhang, *Cell* **74**, 1135 (1993).
12. A. Bonni, D. A. Frank, C. Schindler, M. E. Greenberg, *Science* **262**, 1575 (1993).
13. H. Kotanides and N. C. Reich, *ibid.*, p. 1265.
14. Z. Zhong, Z. Wen, J. E. Darnell Jr., *Proc. Natl. Acad. Sci. U.S.A.*, in press.
15. K. Yamamoto *et al.*, unpublished results.
16. We searched for STAT family members in mouse cells and tissues because of the easy availability of differentiated cell material. With a pair of primers based on the DNA sequence of the SH2 domain of Stat1, we amplified and cloned an ~300-bp fragment of the mouse Stat1 cDNA and then selected the whole cDNA. Comparison of the entire human and mouse Stat1 sequences verified strong similarity of both amino acid (>95%) and nucleic acid sequences (~90%) throughout the entire coding region.
17. GenBank accession numbers for the sequences are U06922 for Stat3, U06923 for Stat4, and U06924 for mouse Stat1.
18. D. Lew, T. Decker, I. Strehlow, J. E. Darnell Jr., *Mol. Cell. Biol.* **11**, 182 (1991); R. N. Pearse, R. Feinman, K. Shuai, J. E. Darnell Jr., J. V. Ravetch, *Proc. Natl. Acad. Sci. U.S.A.* **90**, 4314 (1993).
19. B. J. Wagner, T. E. Hayes, C. J. Hoban, B. H. Cochran, *EMBO J.* **9**, 4477 (1990).
20. T. Akiyama *et al.*, *J. Biol. Chem.* **262**, 5592 (1987).
21. U. M. Wegenka, J. Buschman, C. Lutticken, P. C. Heinrich, F. Horn, *Mol. Cell. Biol.* **13**, 276 (1993).
22. C. Lütticken *et al.*, *Science* **263**, 89 (1994).
23. X.-Y. Fu, D. S. Kessler, S. A. Veals, D. E. Levy, J. E. Darnell Jr., *Proc. Natl. Acad. Sci. U.S.A.* **87**, 8555 (1990).
24. F. M. Ausubel *et al.*, Eds., *Current Protocols In Molecular Biology* (Wiley, New York, 1993).

25. We thank X. Qin, W. Swiggard, and M. Nussenzweig for the mouse thymus library and W. Chen for the Rc/CMV vector. Supported by NIH grant AI32489 (J.E.D.).

21 December 1993; accepted 24 February 1994

Formation of Nascent Intercalated Disks Between Grafted Fetal Cardiomyocytes and Host Myocardium

Mark H. Soonpaa, Gou Young Koh, Michael G. Klug, Loren J. Field*

Fetal cardiomyocytes isolated from transgenic mice carrying a fusion gene of the α-cardiac myosin heavy chain promoter with a β-galactosidase reporter were examined for their ability to form stable intracardiac grafts. Embryonic day 15 transgenic cardiomyocytes delivered directly into the myocardium of syngeneic hosts formed stable grafts, as identified by nuclear β-galactosidase activity. Grafted cardiomyocytes were observed as long as 2 months after implantation, the latest date assayed. Intracardiac graft formation did not induce overtly negative effects on the host myocardium and was not associated with chronic immune rejection. Electron microscopy revealed the presence of nascent intercalated disks connecting the engrafted fetal cardiomyocytes and the host myocardium. These results suggest that intracardiac grafting might provide a useful approach for myocardial repair, provided that the grafted cells can contribute to myocardial function.

It is widely accepted that the adult mammalian myocardium has no regenerative capacity (*1*). As a consequence, cardiomyocyte loss as a result of injury or disease is irreversible. The ability to graft healthy myocytes into a diseased heart might compensate for myocardial loss, provided that the grafted cells are able to couple with host myocytes.

The feasibility of intracardiac grafting was first established with AT-1 cardiomyocytes, a differentiated tumor cell lineage derived from transgenic mice expressing the SV40 large T antigen (*2*). AT-1 cardiomyocytes formed stable grafts when introduced into the myocardium of syngeneic hosts, and graft formation did not overtly impair host heart function (*3*). However, no coupling was observed between grafted AT-1 cardiomyocytes (derived from the atria of transgenic mice) and host ventricular cardiomyocytes. Furthermore, because AT-1 cardiomyocytes are transformed, their ability to effect long-term myocardial repair is limited. Subsequent studies have assessed the capacity of skeletal myoblasts to form stable intracardiac grafts. C2C12 myoblasts delivered into the myocardium of syngeneic hosts differentiated to form grafts comprised of fused, multinucleated myotubes that were stable for at least 6 months (*4*). Furthermore, graft myocytes stopped cell cycling by 1 month after implantation, as measured by [^{3}H]thymidine incorporation. Surface electrocardiographic and plasma enzyme analyses did not detect any overtly negative effects on the host heart. However, it was not clear if the grafted C2C12 myocytes were able to couple to host cardiomyocytes, a prerequisite for this approach to successfully repair a diseased heart.

To explore further the use of intracardiac grafting as a means to effect myocardial repair, we generated transgenic mice that carry a fusion gene comprised of the α-cardiac myosin heavy chain (MHC) promoter and a modified β-galactosidase (β-gal) reporter (nLAC) (*5*). The nLAC reporter carries the SV40 nuclear transport signal, which results in the accumulation of β-gal activity in the nucleus of targeted cells. Four transgenic lineages were produced, and two (designated MHC-nLAC-2 and MHC-nLAC-4) were selected for further analyses. To ensure that the MHC-nLAC transgene would provide a suitable cell lineage marker, we assessed β-gal activity in transgenic cardiomyocytes. Single cell preparations generated by retrograde collagenase perfusion (*6*) were examined simultaneously for β-gal activity and 4,6-diamino-2-phenylindole (DAPI) epifluorescence (Fig. 1, A and B). Almost all (99.0 ± 0.45%, n = 400 for MHC-nLAC-2 and 100.0 ± 0.00%, n = 200 for MHC-nLAC-4) of the transgenic cardiomyocyte nuclei expressed β-gal, whereas no β-gal activity was detected in noncardiomyocytes. In addition, no nuclear β-gal activity was detected in nontransgenic control cardiomyocytes.

Single cell suspensions were prepared by collagenase digestion of hearts harvested from embryonic day 15 MHC-nLAC-2 or MHC-nLAC-4 transgenic mice (*7*). Greater than 95% of the cardiomyocytes isolated by this technique were viable, as evidenced by dye exclusion assay. Cardiomyocytes were delivered to the left ventricular free wall of syngeneic nontransgenic animals (*8*). Grafted cardiomyocytes were readily and unambiguously identified by virtue of the nuclear β-gal activity encoded by the MHC-nLAC transgene (Fig. 1, C and D). Grafted cardiomyocytes

Krannert Institute of Cardiology, Indiana University School of Medicine, 1111 West 10th Street, Indianapolis, IN 46202–4800, USA.

*To whom correspondence should be addressed.